J Nanopart Res (2011) 13:6545–6553
DOI 10.1007/s11051-011-0559-9

RESEARCH PAPER

Magnetic nanoparticles for a new drug delivery system to control quercetin releasing for cancer chemotherapy

A. C. H. Barreto · V. R. Santiago · S. E. Mazzetto · J. C. Denardin · R. Lavín · Giuseppe Mele · M. E. N. P. Ribeiro · Icaro G. P. Vieira · Tamara Gonçalves · N. M. P. S. Ricardo · P. B. A. Fechine

Received: 25 September 2010 / Accepted: 22 August 2011 / Published online: 3 September 2011

Abstract Quercetin belongs to the chemical class of flavonoids and can be found in many common foods, such as apples, nuts, berries, etc. It has been demonstrated that quercetin has a wide array of biological effects that are considered beneficial to health treatment, mainly as anticancer. However, therapeutic applications of quercetin have been restricted to oral administration due to its sparing solubility in water and instability in physiological medium. A drug delivery methodology was proposed in this work to study a new quercetin release system in the form of magnetite–quercetin–copolymer (MQC). These materials were characterized through XRD, TEM, IR, and Thermal analysis. In addition, the magnetization curves and quercetin releasing experiments were performed. It was observed a nanoparticle average diameter of 11.5 and 32.5 nm at Fe_3O_4 and MQC, respectively. The presence of magnetic nanoparticles in this system offers the promise of targeting specific organs within the body. These results indicate the great potential for future applications of the MQC to be used as a new quercetin release system.

Keywords Drug delivery · Quercetin · Magnetic nanoparticles · Copolymer · Nanomedicine

A. C. H. Barreto · V. R. Santiago · P. B. A. Fechine (✉)
Grupo de Química de Materiais Avançados (GQMAT),
Departamento de Química Analítica e Físico-Química,
Universidade Federal do Ceará – UFC, Campus do Pici,
CP 12100, Fortaleza, CE 60451-970, Brazil
e-mail: fechine@ufc.br

A. C. H. Barreto · V. R. Santiago · S. E. Mazzetto
Laboratório de Produtos e Tecnologia em Processos—
LPT, Departamento de Química Orgânica e Inorgânica,
Universidade Federal do Ceará, Fortaleza, CE, Brazil

J. C. Denardin · R. Lavín
Departamento de Física, Universidad de Santiago de
Chile, USACH, Av. Ecuador, 3493 Santiago, Chile

R. Lavín
Facultad de Ingeniería, Universidad Diego Portales,
Ejército 441, Santiago, Chile

G. Mele
Dipartimento di Ingegneria dell'Innovazione, Università
del Salento, 73100 Via Arnesano, LE, Italy

M. E. N. P. Ribeiro · N. M. P. S. Ricardo
Departamento de Química Orgânica e Inorgânica,
Universidade Federal do Ceará, CX 6.021, Fortaleza, CE
60455-760, Brazil

I. G. P. Vieira
Parque de Desenvolvimento Tecnológico (PADETEC),
Campus do Pici, Fortaleza, CE 60455-970, Brazil

T. Gonçalves
Departamento de Farmácia, Universidade Federal do
Ceará, Fortaleza, CE, Brazil

Introduction

Flavanoids have been associated with a variety of biochemical and pharmacological properties, including antibacterial, antiallergic, antimutagenic, anticarcinogenic, antiviral, antineoplastic, anti-inflammatory, anti-thrombotic, vasodilator, scavenger, and antioxidant activities and are believed to be beneficial to human health (Bukhari et al. 2008).

Quercetin, 3,3′,4′,5′-7- pentahydroxy flavone belongs to the chemical class of flavonoids and is widely distributed in vegetables and plants (Ribeiro et al. 2009). It is commonly found in many foods, including apples, tea, onions, nuts, berries, cauliflower, and cabbage. It has been demonstrated that quercetin possesses a wide variety of biological effects that are considered beneficial to health, including antioxidative, free radical scavenging, antiviral activities, and mainly anticancer (Zheng et al. 2005; Kumari et al. 2010). However, therapeutic applications of quercetin have been restricted to oral administration due to its sparing solubility in water and instability in physiological medium (Zheng et al. 2005; Kumari et al. 2010). A useful response has been the development of colloidal magnetic delivery systems based on amphiphilic block copolymers, whose micelles can accommodate poorly soluble guest molecules (Pinho et al. 2007; Ribeiro et al. 2009; Wei et al. 2009).

Recently, magnetic nanoparticles, mainly Fe_3O_4, have generated a lot of interest in biomedical applications for magnetic resonance imaging, magnetic separation, targeted drug delivery, tissue engineering, cell tracking, bioseparation, and magnetic hyperthermia (Giri et al. 2008; Shubayev et al. 2009). For these applications, the particles must have high magnetic saturation, biocompatibility, and interactive functions at the surface.

Studies in vivo have shown that Fe_3O_4 nanoparticles are relatively safe as they do not accumulate in the vital organs and are rapidly eliminated from the body (Boyer et al. 2010; Doraiswamy and Finefrock 2004). The presence of a polymer coating, such as polyethylene glycol (PEG), can also mediate Fe_3O_4 toxicity, as demonstrated for human fibroblasts (Gupta and Curtis 2004; Wang et al. 2008). In this way, several approaches have been developed to coat iron oxide nanoparticles during the synthesis (in situ) and post-synthesis. In the literature, the most common coatings are PEG, polyvinyl alcohol (PVA), dextran, alginate, and chitosan (Laurent et al. 2008).

Magnetic drug targeting employing nanoparticles as carriers is a promising cancer treatment avoiding the side effects of conventional chemotherapy. Alexiou et al. (2006) have shown that a strong magnetic field gradient at the tumor location induces accumulation of the nanoparticles. Several reports have been published on the use of Fe_3O_4 nanoparticles as nanocarriers for drug delivery. A study carried out by Gallo et al. (1993) has shown that, after administration of magnetic microspheres containing oxantrazole, the brain contained 100–400 times higher oxantrazole levels than those obtained after the solution dosage form, indicating the success of drug delivery via magnetic particles. Therefore, the load and release of bioactive materials from the polymer coating then becomes a significant parameter dictating the efficiency of IONPs as nanocarriers.

In this article, we present the results of a new approach to quercetin storage and release using magnetite nanoparticles (Fe_3O_4). This system was incorporated to a triblock copolymer of ethylene oxide and oxyphenylethylene, type $E_{137}S_{18}E_{137}$ (where E denotes oxyethylene, OCH_2CH_2, S denotes oxyphenylethylene, $OCH_2CH(C_6H_5)$, and the subscripts denote number-average block lengths in chain units). In addition, we also focused on a quercetin release from copolymer as a drug carrier system for anticancer agents.

Experimental

Materials

The chemical reagents for this study are $FeCl_3{\cdot}6H_2O$ (pure granulated 99%), $FeSO_4{\cdot}7H_2O$ (pure granulated 99%), and 30% ammonia solution. Copolymer $E_{137}S_{18}E_{137}$ ($M_n = 14200$ g mol^{-1}, $M_n/M_w = 1.06$, weight fraction E, $w_E = 0.85$, cmc = 23 mg L^{-1}) was prepared in Manchester laboratory. Details can be found elsewhere (Yang et al. 2003; Pinho et al. 2007). Quercetin was supplied by Flora Brasil Ltd. Water was Milli-Q quality, chloroform and methanol were synthesis graded.

Table 1 The composition and concentration of materials used in nanoparticles formulations

Formulation	Magnetite–quercetin (% w/w)		MQC (% w/w)	
	Quercetin	Fe_3O_4	MQ	$E_{137}S_{18}E_{137}$
F1	1	3	–	–
F2	1	5	–	–
F3	1	10	–	–
F4	–	–	F2	3
F5	–	–	F2	5
F6	–	–	F2	10

Synthesis of magnetite nanoparticles

In the co-precipitation processing route, the solution of metallic salts containing Fe^{2+}/Fe^{3+} was dissolved and mixed in Milli-Q water in the ratio molar of 1:2 to form the spinel phase Fe_3O_4. The aqueous mixtures were heated to 80 °C and then added into a 30 wt% NH_4OH solution was subjected to vigorous stirring until pH 10 to form a black precipitate. The precipitate was washed several times with Milli-Q water until the residual solution became neutral. Finally, the magnetic nanoparticles were dried. The chemical reaction of Fe_3O_4 formation may be written as Eq. 1.

$$Fe^{2+} + 2Fe^{3+} + 8OH^- \rightarrow Fe_3O_4 + 4H_2O \quad (1)$$

Preparation of new magnetic drug delivery

A new magnetic drug delivery was prepared by the emulsion-coacervation method (Hu et al. 2006) followed by coating with a solution composed of polymer. In addition, it can be stabilized by physical intermolecular or covalent cross-linking, which typically can be achieved by altering pH or temperature, or by adding a cross-linking agent.

Several formulations were tested and the compositions are as shown in Table 1. The proportions of the composition Quercetin:Magnetite (MQ) were 1:3 (F1), 1:5 (F2), and 1:10 (F3) (given in Table 1). FTIR analysis was used to study the effect of drug loading and the identification of encapsulated chemical on the release characteristics of the drug. After FTIR analysis, the batch F2 showed the best results. The next step was to coat the batch F2 with copolymer. The proportions of the composition for MQ:copolymer used were 1:5:1 (F4), 1:5:5 (F5), and 1:5:10 (F6). And after the FTIR analysis, the Batch F5 was chosen as the best batch (given in Table 1).

Quercetin (100 mg) was dissolved in methanol. NH_4OH solution was then added until pH >7, to remove the hydrogen of the phenolic groups. 20 mg of Fe_3O_4 was injected into the mixture. This resulting mixture was kept under stirring at room temperature for 1 h. After reaction, the solvent was extracted and the powder was kept in desiccator for 2 days to remove water that appeared as sub-product from the reaction. Schematic illustration of the reaction is represented in Fig. 1. This reaction was chosen following the study of Bukhari et al. (2008). They proposed a quercetin linkage to a metal to form the

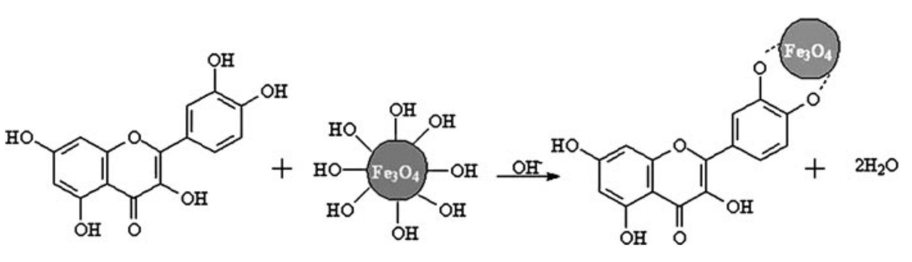

Fig. 1 Proposed structured of the Fe_3O_4–quercetin complex

metal–quercetin complex. Cheng et al. (2009) made similar synthesis linking cisplatin in polymer.

The presence of hydroxyl groups, such as Fe–OH, on magnetic nanoparticles surface provides a versatile synthetic handle allowing attachment of different functionalities. In aqueous solutions, the Fe atoms coordinate with water, which readily dissociate to leave the iron oxide surface hydroxyl functionalized. These hydroxyl groups are amphoteric and may react with acids or bases (Laurent et al. 2008).

It was necessary to make a coating on magnetite–quercetin (MQ) with copolymer $E_{137}S_{18}E_{137}$ to obtain a magnetic colloidal suspension that was reasonably stable against aggregation in both biological medium and magnetic field. In order to prepare MQ incorporated to the copolymer (MQC), it was needed 20 mg of MQ dissolved in chloroform and then 100 mg of copolymer $E_{137}S_{18}E_{137}$ was added in the solution. The mixture was kept under stirring at room temperature for 2 h. After this reaction, the solvent was extracted and the solid was characterized. The stabilization of the system was achieved through the method of preparation and the type of the triblock polymer used.

Quercetin releasing from copolymer $E_{137}S_{18}E_{137}$

MQC samples were resuspended in PBS (pH = 7.4) and then transferred into a dialysis bag. The bag was placed into the same buffered solution (25 mL). The release study was performed at 37 ± 0.5 °C. At predetermined time intervals, 3 mL of the aqueous solution were withdrawn and replenished with 3 mL of fresh buffer solution. The amount of drug release was measured through the absorbance using UV spectrophotometer at 375 nm for quercetin (initial drug concentration in dialysis bag was 40 µg/mL). In the assessment of drug release behavior, the cumulative amount of released drug was calculated and the percentages of quercetin released from the copolymer were plotted against time. A U-2000 Spectrophotometer by Hitachi was used in the analysis.

Characterization

The X-ray diffraction (XRD) analysis was performed in an X-ray powder diffractometer Xpert Pro MPD (Panalytical) using Bragg–Brentano geometry in the range of 20°–120° with a rate of 1° min^{-1}. CoKα radiation ($\lambda = 1.7889$ Å) was used and the tube operated at 40 kV and 30 mA. The phase identification analysis was made by comparing powder diffractograms with standard patterns from International Centre for Diffraction Data (ICDD). For the magnetic nanoparticles, the experimental patterns were numerically fitted with the Rietveld algorithm in a procedure to better identify and quantify crystallographic phases.

The infrared measurements were performed using a Perkin Elmer 2000 spectrophotometer in the 400–4000 cm^{-1} range. The samples were previously dried and grounded to powder and pressed (10 µg of sample to 100 mg of KBr) in disk format for measurements.

The magnetization measurements were performed at room temperature with a home-made vibrating sample magnetometer (VSM). The VSM has previously been calibrated using a pure Ni wire, and after measuring the mass of each sample the magnetization was given in emu/g.

The thermal stability of the nanoparticle Fe_3O_4 and magnetic drug was done by Mettler Toledo TGA/SDTA 851^e machine. The analysis was performed under nitrogen atmospheres in constant flow of 50 cm^3 min^{-1}, with heating range of 10 °C min^{-1}, sample mass of 10 mg, and temperature programs from 30 to 800 °C.

Low-magnification TEM analysis was performed on a Jeol JEM-1011 electron microscope operating at 100 kV, equipped with a CCD camera ORIUS 831 from Gatan. TEM samples were prepared by drop-casting dilute nanocrystal solutions onto carbon coated copper grids. Afterward, the deposited samples were allowed to dry completely, at 60 °C, for one night, before examination.

Results and discussion

In this study, six batches of nanoparticles were prepared using different ratios of magnetite and copolymer. Table 1 summarizes the composition of the batches that have been studied. This table shows the attempt to obtain the best conditions of the drug delivery system. However, due the limited amount of the sample we could not do enough experiments to allow us statistical discussions. After FTIR analysis, the formulation F2 was selected for covering with

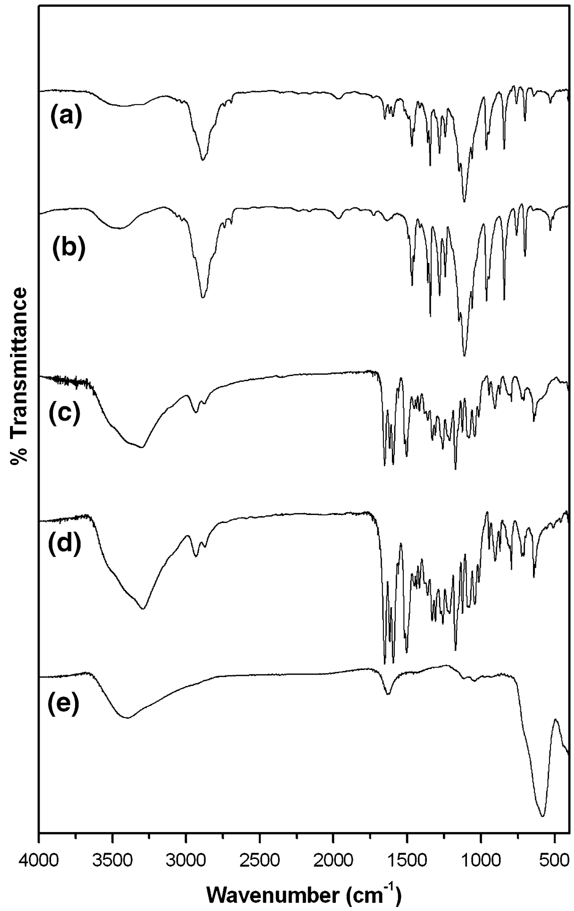

Fig. 2 FTIR analysis of *a* Fe_3O_4, *b* quercetin, *c* Fe_3O_4–quercetin, *d* Triblock copolymer $E_{65}S_{19}E_{65}$, *e* Fe_3O_4–quercetin–copolymer

different ratios of $E_{137}S_{18}E_{137}$. The increase in polymer concentration is one of the factors affecting the drug release rate from the system. The results showed that the formulation F5 presented the highest encapsulation efficiency.

FTIR analysis is one of the most important techniques for the quick and efficient identification of encapsulated chemical molecules (Kumari et al. 2010). In Fig. 2a, it was observed characteristic peaks of Fe–O at 580 cm^{-1} for Fe_3O_4 as the main phase of spinel ferrites and corresponds to stretching vibration in tetrahedral site (Hrdina et al. 2010; Slavov et al. 2010). Fe_3O_4 has the general molecular formula $(Fe^{2+})[Fe^{3+}]O_4^{2-}$ where the divalent and trivalent cations occupying tetrahedral (Fe^{2+}) and octahedral [Fe^{3+}] interstitial positions of the fcc lattice are formed by O^{2-} ions (Chinnasamy et al. 2001). The presence of hydroxyl groups that reside at the nanoparticles surface (Fig. 1) was observed in the broad absorption of O–H stretching at 3411 cm^{-1} for Fe_3O_4 and the peak at 1637 cm^{-1} is due to angular vibration of O–H. Owing to the fact that synthesis of the spinel ferrites was performed in aqueous solution, the surface materials were covered by hydroxyl groups from water, so that the IR spectrum showed these bands.

Figure 2b shows characteristic vibration modes for quercetin of C=O stretching (1654 cm^{-1}) and –OH stretching phenolic (3304 cm^{-1}). The band at 641 cm^{-1} represents phenolic ring bending of quercetin. This signal is enlarged with addition of magnetite (Fig. 2c). It was observed that the absorption band in O–H at 3304 cm^{-1} decreases in intensity due to the removal of phenolic hydrogen and input of Fe_3O_4 nanoparticles, confirming a new linking between drug and Fe_3O_4 (see Fig. 1). Figure 2d represents IR spectrum for copolymer with main bands at 1114 cm^{-1} associated to the linking aliphatic ether (R–O–R′) and 2881 cm^{-1} associated to aliphatic chain. In Fig. 2e, it was not observed the signal of the linking Fe–O due to superposition of bands and coverage of quercetin and copolymer on Fe_3O_4 (MQC). However, one can observe the absorption at 1654 cm^{-1} assigned C=O of quercetin. This band is absent in copolymer (Fig. 2d) and confirms the quercetin encapsulation.

To determine the amount of quercetin and copolymer that can be associated to the magnetite surface, thermogravimetric analysis was used to determine the mass loss of the magnetite in comparison with magnetite coated quercetin and copolymer–quercetin (Fig. 3). The magnetite amounts from samples can be estimated from the residual mass percentages. The

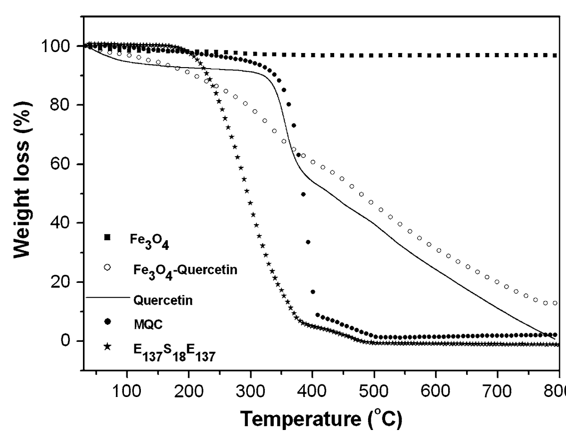

Fig. 3 Weight loss by thermogravimetric analysis

magnetite curve (Fig. 3) shows that weight loss over the temperature range from 30 to 800 °C is about 9%. This might be due to loss of adsorbed physical and chemical water in the nanoparticle surface, as it was observed in FTIR analysis (see Fig. 2a). For Fe_3O_4 nanoparticles chelate to quercetin, the weight loss residual range from 30 to 800 °C is about 13%. This data reflect the decomposition of organic components complexion to the nanoparticles surface. However, both quercetin and copolymer ($E_{137}S_{18}E_{137}$) thermograms showed that weight loss over the temperature range from 30 to 800 °C was total. Some studies (Rohn et al. 2007; Makris and Rossiter 2000) mentioned that quercetin glycosides where quercetin is degraded to several products during heating using aqueous conditions at around 100 °C. However, quercetin is not sensitive to degradation under such conditions and therefore has to be regarded as a stable end product. For quercetin curve (Fig. 3), there are two stages: The first (at about 100 °C) is the water loss, and the second corresponds to the initial decomposition process for the quercetin (Costa et al. 2002). These stages were not observed in Fe_3O_4 chelate to quercetin, confirming that there was change in the molecule, as shown in Fig. 3.

The TGA data demonstrated that the weight loss in MQC occurs at about 300 °C (range 280–430 °C), which is higher than that for the pure copolymer (180 °C, range 160–390 °C) (Fig. 3). This shift in the temperature could be due to chemisorption of quercetin and copolymer multilayer on magnetite nanoparticle surface, requiring higher temperature for the degradation of sample. For MQC, the weight loss residual range from 30 to 800 °C is about 3%.

The size and morphology of Fe_3O_4 nanoparticles were observed by Transmission Electron Microscopy (TEM), as shown in Fig. 4a, b. Fe_3O_4 nanoparticles maintain a typical spherical shape and the particle size of magnetite ranged from 13 ± 2 nm grown in a flower-like arrangement. They are polydisperse and some of them agglomerated due to magneto-dipole interactions between particles. This kind of behavior has been observed in other studies (Zhao et al.2009; Rao et al. 2007; Wang et al. 2005).

The crystalline structure and nanoparticle size of Fe_3O_4 were investigated by XRD analysis (Fig. 5). The diffraction patterns for magnetite showed that all the reflection peaks at {111}, {220}, {311}, {400}, {422}, {511}, {440}, {533}, and {553} can be well indexed to the inverse cubic spinel structure of Fe_3O_4 (JCPDS card # 08-4611) with spatial group F*d*3M. These results confirm that the nanoparticles synthesized in this study are the Fe_3O_4. The crystal size was calculated using the Scherrer's equation (Braga et al. 2010). These results show that the average size of magnetite nanoparticles was about 11 nm, which agrees with the size determined by TEM (see Fig. 4).

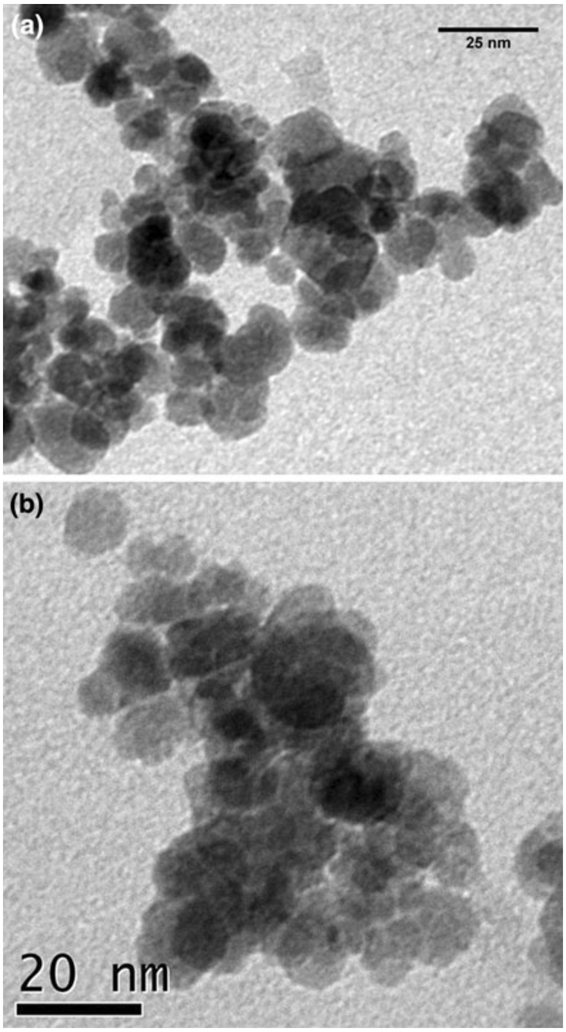

Fig. 4 TEM images of Fe_3O_4 nanoparticles

VSM was performed to investigate the magnetic properties of the Fe_3O_4 and MQC at room temperature. In Fig. 6, the hysteresis loops that are characteristic of superparamagnetic behavior can be observed for Fe_3O_4 nanoparticles. There is no hysteresis in the magnetization curve with both remanence and coercivity being zero, indicating that

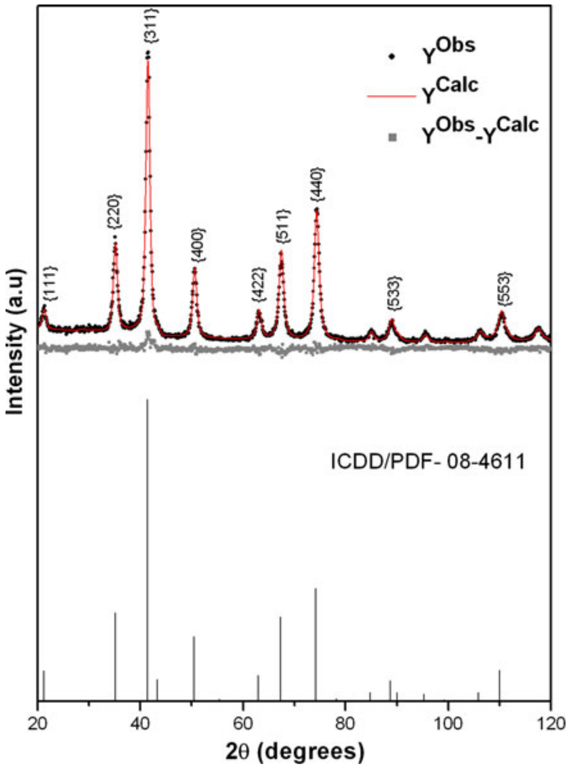

Fig. 5 XRD patterns of the Fe_3O_4 nanoparticles

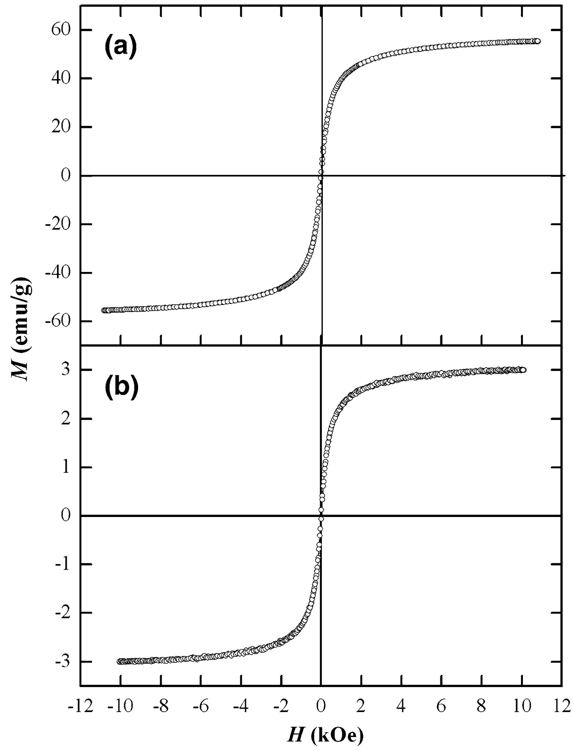

Fig. 6 Magnetization curves of **a** pure Fe_3O_4 and **b** MQC

these magnetic nanoparticles are superparamagnetic. This feature is an important property needed for magnetic targeting carriers, because capillary blockage by aggregations formed by residue magnetism after removal of the applied field will be avoided (Hu et al. 2006). The saturation magnetization of MQC is found to be 3 emu/g. This value is lower than that for magnetite nanoparticles (55 emu/g) because of the two coating layers of quercetin and copolymer. This feature allows the nanoparticles for highly efficient magnetic manipulation when used as drug delivery (Cao et al. 2009). The novelty of this study resides in the fact that it presents the possibility of the displacement control by use of the magnetic field. This is the first time that this type of system is proposed and it can be important for targeted drug delivery and for drug releasing.

The hysteresis curve (Fig. 7) $M(H)$ at room temperature of these samples can be well described by a Langevin function, $M/M_0 = \coth(\mu H/k_B T) - k_B T/\mu H$ with μ representing the magnetic moment, H the external magnetic field, T the temperature, and k_B the Boltzmann constant. The particle size can be inferred from this Langevin function adjusting the parameter $a = \mu/k_B$ which is related with the diameter of the particle as $a = 4\pi(d/2)^3 M_0/3k_B$ with d being the diameter of the particle. Thus, using this fitting with parameters a of 1 and 1.3 gives us an average diameter of 11.5 and 32.5 nm at Fe_3O_4 and MQC, respectively. This result agrees with the size determined for magnetite by DRX and TEM (see Figs. 4, 5, respectively).

The quercetin release from MQC was pH-dependent, as shown in Fig. 8. In the first 10 h, there was an initial rapid burst release. This fact is normally attributed to the fraction of quercetin which was adsorbed in the surface of the copolymer (Kumari et al. 2010). The cumulative release of quercetin as a diffusion controlled process under a physiological condition (pH 7.4) shows a gradual increase and reaches a plateau after 48 h with release of 13.5% of the quercetin.

The release of quercetin achieved its peak at 14.5% after 96 h. In early stage of release, an initial burst effect was observed. This behavior was probably due to the small amount of poorly encapsulated

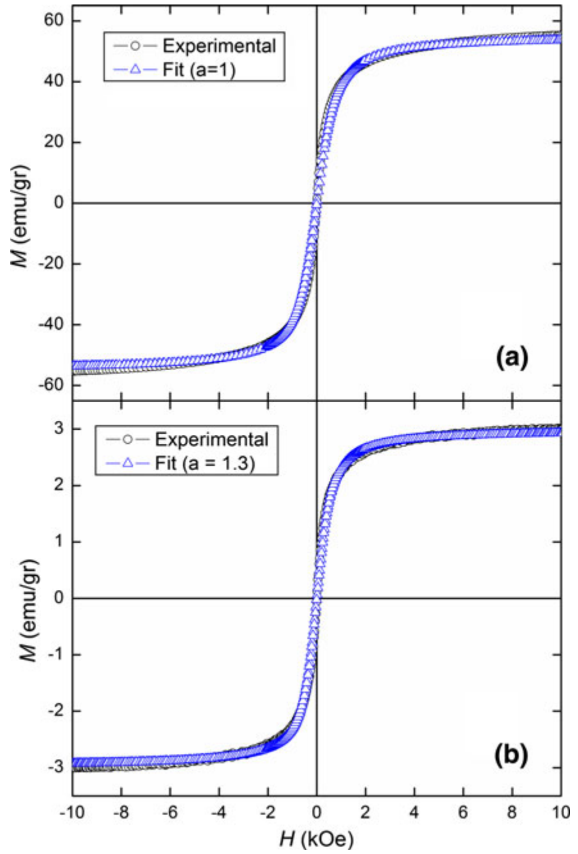

Fig. 7 Magnetization curves of **a** pure Fe_3O_4 and **b** MQC adjusted by Langevin function

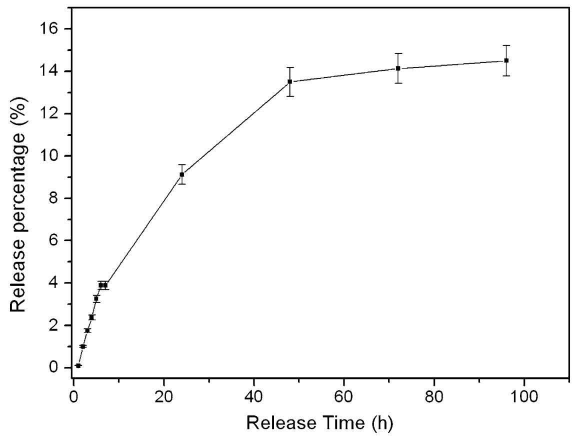

Fig. 8 Release profile of quercetin from Fe_3O_4–quercetin–copolymer by UV–Vis method

quercetin bound to the nanoparticle surface. It is believed that the small amount of drug release is due to the strong interaction between nanoparticles of magnetite and quercetin that make the drug release more difficult.

Conclusions

We prepared Fe_3O_4 nanoparticles by co-precipitation route in the range of 10–15 nm. This size was confirmed by TEM, XRD, and hysteresis curve (Langevin function). For MQC system, it was found a size of 32.5 nm due to the copolymer covered. Fe_3O_4 was linked to quercetin with the objective of targeted delivery and the novel approach using quercetin was characterized by FTIR and TGA. These results and data from literature were used to propose a magnetite–quercetin interaction. This biomaterial was encapsulated on triblock copolymer ($E_{137}S_{18}E_{137}$) for drug delivery and controlled release of the cancer chemotherapeutic. The presence of magnetic nanoparticles presented in this system offers the promise of being able to target specific organs within the body. In the current form, the MQC system showed that there is a prolonged release time (its peak at 14.5% after 96 h) for the drug. However, changes in the system composition could adequate to an ideal release time. These results indicate the great potential for future applications of the MQC to be used as a new quercetin release system.

Acknowledgments The authors thank Dr. Zhuo Yang for the preparation and characterization of copolymer $E_{137}S_{18}E_{137}$. The study was supported by CAPES, Funcap and CNPq (Brazilian agencies). Financiamiento Basal para Centros Cientificos y Tecnologicos de Excelencia CEDENNA), Millennium Science Nucleus Basic and Applied Magnetism (P06-022F) and Fondecyt 1080164 and 3100117.

References

Alexiou C et al (2006) Targeting cancer cells: Magnetic nanoparticles as drug carriers. Eur Biophys J 35:446–450

Boyer C, Whittaker MR, Bulmus V, Liu J, Davis TP (2010) The design and utility of polymer-stabilized iron-oxide nanoparticles for nanomedicine applications. NPG Asia Mater 2:23–30

Braga TP, Vasconcelos IF, Sasaki JM, Fabris JD, Oliveira DQL, Valentini A (2010) Magnetic composites based on hybrid spheres of aluminum oxide and superparamagnetic nanoparticles of iron oxides. J Magn Magn Mater 322: 633–637

Bukhari SB, Memon S, Tahir MM, Bhanger MI (2008) Synthesis, characterization and investigation of antioxidant activity of cobalt–quercetin complex. J Mol Struct 892:39–46

Cao H, He J, Deng L, Gao X (2009) Fabrication of cyclodextrin-functionalized superparamagnetic Fe_3O_4/amino-silane core-shell nanoparticles via layer-by-layer method. Appl Surf Sci 255:7974–7980

Cheng K, Peng S, Xu C, Sun S (2009) Porous hollow Fe_3O_4 nanoparticles for targeted delivery and controlled release of cisplatin. J Am Chem Soc 131:10637–10644

Chinnasamy CN et al (2001) Mixed spinel structure in nanocrystalline $NiFe_2O_4$. Phys Rev B 63:184108

Costa EM, Filho JMB, Nascimento TG, Macedo RO (2002) Thermal characterization of the quercetin and rutin flavonoids. Thermochim Acta 392–393:79–84

Doraiswamy PM, Finefrock AE (2004) Metals in our minds: therapeutic implications for neurodegenerative disorders. Lancet Neurol 3:431–434

Gallo JM, Varkonyi P, Hassan EE, Groothius DR (1993) Targeting anticancer drugs to the brain: II. physiological pharmacokinetic model of oxantrazole following intraarterial administration to rat glioma-2 (RG-2) bearing rats. J Pharm Biopharm 21:575–592

Giri J et al (2008) Synthesis and characterizations of water-based ferrofluids of substituted ferrites [Fe1-xBxFe2O4, B = Mn, Co (x = 0–1)] for biomedical applications. J Magn Magn Mater 320:724–730

Gupta AK, Curtis ASG (2004) Surface modified superparamagnetic nanoparticles for drug delivery: interaction studies with human fibroblasts in culture. J Mater Sci Mater Med 15:493–496

Hrdina A, Lai E, Li C, Sadi B, Kramer G (2010) A comparative study of magnetic transferability of superparamagnetic nanoparticles. J Magn Magn Mater 322:2622–2627

Hu FX, Neoh KG, Kang ET (2006) Synthesis and in vitro anticancer evaluation of tamoxifen-loaded magnetite/PLLA composite nanoparticles. Biomaterials 27:5725–5733

Kumari A, Yadav SK, Pakade YB, Singh B, Yadav SC (2010) Development of biodegradable nanoparticles for delivery of quercetin. Colloids Surf B 80:184–192

Laurent S et al (2008) Magnetic iron oxide nanoparticles: synthesis, stabilization, vectorization, physicochemical characterizations, and biological applications. Chem Rev 108:2064–2110

Makris DP, Rossiter JT (2000) Heat-induced, metal-catalyzed oxidative degradation of quercetin and rutin (quercetin 3-o-rhamnosylglucoside) in aqueous model systems. J Agric Food Chem 48:3830–3838

Pinho MEN, Costa FMLL, Filho FBS, Ricardo NMPS, Yeates SG, Attwood D, Booth C (2007) Mixtures of triblock copolymers $E_{62}P_{39}E_{62}$ and $E_{137}S_{18}E_{137}$ potencial for drug delivery from in situ gelling micellar formulations. Int J Pharm 328:95–98

Rao BP, Rao GSN, Kumar AM, Rao KH, Murthy YLN, Hong SM, Kim CO, Kim C (2007) Soft chemical synthesis and characterization of $Ni_{0.65}Zn_{0.35}Fe_2O_4$ nanoparticles. J Appl Phys 101:123902-1–123902-4

Ribeiro MENP, Vieira IGP, Cavalcante IM, Ricardo NMPS, Attowood D, Yeates SG, Booth C (2009) Solubilisation of griseofulvin, quercetin and rutin in micellar formulations of triblock copolymers $E_{62}P_{39}E_{62}$ and $E_{137}S_{18}E_{137}$. Int J Pharm 378:211–214

Rohn S, Buchner N, Driemel G, Rauser M, Kroh LW (2007) Thermal degradation of onion quercetin glucosides under roasting conditions. J Agric Food Chem 55:1568–1573

Shubayev VI, Pisanic TR II, Jin S (2009) Magnetic nanoparticles for theragnostics. Adv Drug Deliv Rev 61:467–477

Slavov L et al (2010) Raman spectroscopy investigation of magnetite nanoparticles in ferrofluids. J Magn Magn Mater 322:1904–1911

Wang Z, Shen B, Aihua Z, He N (2005) Synthesis of Pd/Fe_3O_4 nanoparticle-based catalyst for the cross-coupling of acrylic acid with iodobenzene. Chem Eng J 113:27–34

Wang Y et al (2008) Formulation of superparamagnetic iron oxides by nanoparticles of biodegradable polymers for magnetic resonance imaging. Adv Funct Mater 18:308–318

Wei X, Gong C, Gou M, Fu S, Guo Q, Shi S, Luo F, Qiu L, Qian Z (2009) Biodegradable poly (ε-caprolactone)-poly(ethylene glycol) copolymers as drug delivery system. Int J Pharm 381:1–18

Yang Z, Crothers M, Ricardo NMPS, Chaibundit C, Taboada P, Mosquera V, Kelarakis A, Havredaki V, Martin L, Valder C, Collett JH, Attwood D, Heatley F, Booth C (2003) Micellisation and gelation of triblock copolymers of ethylene oxide and styrene oxide in aqueous solution. Langmuir 19:943–950

Zhao DL, Zeng XW, Xia QS, Tang JT (2009) Preparation and coercivity and saturation magnetization dependence of inductive heating property of Fe_3O_4 nanoparticles in an alternating current magnetic field for localized hyperthermia. J Alloys Compd 469:215–218

Zheng Y, Haworth IS, Zuo Z, Chow MSS, Chow AHL (2005) Physicochemical and structural characterization of quercetin-β-cyclodextrin complexes. J Pharm Sci 94:1079–1089